Digital image correlation for full-field time-resolved assessment of arterial stiffness

DIGITAL IMAGE CORRELATION FOR FULL-FIELD TIME-RESOLVED ASSESSMENT OF ARTERIAL STIFFNESS

Adriaan Campo[a], Joris Soons[a], Hilde Heuten[b], Guy Ennekens[b], Inge Goovaerts[b], Christiaan Vrints[b], Pascal Lava[c], Joris Dirckx[a]

[a]Bimef; University of Antwerp; Groenenborgerlaan 171 2020 Antwerp Belgium;

[b]Department of Cardiology; University Hospital Antwerp; Wilrijkstraat 10 2650 Edegem Belgium;

[c]Department of metallurgy and materials engineering; KaHo-St.Lieven; Gebroeders De Smetstraat 1 9000 Ghent Belgium.

ABSTRACT

Pulse wave velocity (PWV) of the arterial system is a very important parameter to evaluate cardiovascular health. Currently, however, there is no golden standard for PWV measurement.

In this work, DIC was used for full-field time-resolved assessment of displacement, velocity, acceleration and strains of the skin in the neck directly above the common carotid artery (CCA). By assessing these parameters, propagation of the pulse wave could be tracked, leading to a new method for PWV detection based on DIC.

The method was tested on 5 healthy subjects. As a means of validation, PWV was measured with ultrasound (US) as well. Measured PWV values were between 3,68 m/s and 5,19 m/s as measured with DIC and between 5,14 and 6,58 m/s as measured with US, with a maximum absolute difference of 2,78 m/s between the two methods.

DIC measurements of the neck region can serve as a test base for determining a robust strategy for PWV detection, they can serve as reference for 3D fluid-structure interaction (FSI) models, or they may even evolve into a screening method of their own. Moreover, full-field, time-resolved DIC can be adapted for other applications in biomechanics.

Keywords: digital image correlation, pulse wave velocity, arteriosclerosis

INTRODUCTION

In digital image correlation (DIC), a speckle pattern is physically applied to an object. Coordinates of points, labeled by the randomly applied stochastic (speckled) pattern are captured with a camera and identified with image correlation [1]. These points are followed when the object is deformed and displacements are acquired with sub-pixel resolution. Full-field, three-dimensional surface results can be acquired using a stereo camera system. The optical setup for 3D acquisition consists of 2 cameras and a bright light source only, making this technique easy to deploy and measurements easy to perform. Although image analysis is computationally intensive, increasing computer power has made the technique more popular [2] resulting in biomechanical applications such as strain measurements on human bone and tendon [3], on mouse arteries [4], on mouse bone [5] and on finch beak [6].

In the present work, DIC is applied for the first time, to our knowledge, on a living (human) subject. DIC was used for time-resolved, full field assessment of the movement of the skin in the neck directly above the common carotid artery (CCA). The movement of the skin on this location is directly linked to the pressure inside the CCA [7]. Detecting skin motion on this spot thus allows tracking the pressure wave inside CCA. This pressure wave propagates with a certain velocity, the pulse wave velocity (PWV). PWV of the arterial system is a measure for cardiovascular health [8].

Several methods to measure PWV exist today. Currently, PWV is being measured between the femoral artery (FA) in the groin and the CCA in the neck. For this purpose, there are contact methods based on tonometry [9] or ultrasound (US) [10], or non-contact methods based on laser doppler vibrometry (LDV) [11]. Main advantage of this approach is that it is already well integrated in the clinical circuit. However, the patient is required to be undressed and PWV detection between the neck and the groin, poses specific difficulties [12].

Recently, local PWV of the CCA has attracted serious interest for screening purposes. The CCA is often affected by arteriosclerosis and atherosclerosis [13]. Also, elevated PWV in this part of the arterial system is hypothesized to play a major role in the etiology of cardiovascular disease [14]. Moreover, the easy access of the artery, allows the patient to remain dressed during measurements. Local PWV measurements in the CCA have been realized using US [15,16] and laser doppler vibrometry [17]. However, this approach is relatively new in general, and it lacks validation at the moment.

In this work, DIC is proposed as a screening method on its own for local PWV detection of the CCA. Data acquired with DIC describe full-field, time-resolved deformation of the skin overlaying the CCA. This information can serve as a test base for determining a robust strategy for PWV detection as they create insight in the movements of the skin above the artery and the pressures inside the artery. Moreover they can serve as reference for 3D fluid-structure interaction (FSI) models of the CCA when complete systems including arteries and surrounding tissue and skin are being modeled. Finally, the measurement approach can be adapted easily for other applications in biomechanics such as determination or modeling of biomaterials, study of growth dynamics, amongst other possible examples.

MATERIALS AND METHODS

MEASUREMENT SETUP

A Stereo system with two cameras (Redlake HR1000 and Redlake Motion PRO, IDT, Tallahassee, USA), with 8 bit-depth, resolution of 1280x1024 pixels, and maximum frame rate of 500 fps was used. Cameras were placed at a distance of approximately 1 m from the subject, and mutual distance between cameras was approximately 0,5 m. Both cameras were mounted with an identical 200 mm f/4 lens (Nikon, Tokyo, Japan) with an opening angle of approximately 30 °. Movies were synchronized post hoc, using a short flash from a laser pen. High power LEDs fed with DC to avoid flickering illuminated the sample (See Figure 1). Automatic system calibration was performed by using various images of a translated and rotated regular grid pattern within a bundle adjustment technique taken before, between and after the entire experiment [18,19]. As a result, intrinsic and extrinsic camera parameters were obtained (see Table 1). DIC requires the presence of a random pattern on the specimen. This was applied by air

brushing black paint (Air Stream Makeup Black, Kryolan, Berlin, Germany) on top of a white ground layer (Wet Makeup White, Kryolan, Berlin, Germany) in the left neck region at the level of the left CCA. In order for DIC to perform optimally, the air brushed speckle pattern should have a random character, and the contrast between the speckles and the background should be as high as possible. Without the preparation of the surface, i.e. on the bare skin, DIC will not render satisfying results. 5 young male healthy volunteers participated in this study. Each measurement, a movie of about 1-2 s was recorded with a sample frequency of 500 images per second, in order to capture the movements generated by between 3 and 6 heartbeats (The exact number of recorded heartbeats per subject is given in the results section). The whole measurement was repeated one day later with a different speckle pattern on the same location. In one image, the initial non-deformed shape was reconstructed by finding the corresponding speckles in the images captured by camera 1 and camera 2 and via a triangulation method invoking the determined stereo camera parameters [20]. In the next step, a similar procedure was applied to the subsequent image of the deformed state. Finally, a direct comparison of the deformed (x, y, z) and the undeformed (x0, y0, z0) shape yields the 3D deformation coordinates (u, v, w). These contain all the information needed to determine the in-plane normal and shear strain components (ε_{xx}, ε_{yy}, ε_{xy}), or the principal strains and the shear angle (ε_1, ε_2, γ) as described in [21]. The following settings were used in the displacement determination: a subset size of 16x16 pixels that is being compared between 2 images, a step size of 5 pixels determining the resolution of the correlation analysis, zero-normalized cross-correlation algorithm [22], bicubic interpolation [23] and affine shape functions [24]. Strains were calculated in the Green-Lagrange convention [25] and a strain window of 50x50 pixels and a bilinear interpolation [21] was taken. Results are transformed into the coordinate system of camera 1. All calibration and correlation steps are executed in the MatchID software package (in-house developed: http://www.matchid.org/).

Intrinsic parameters				Extrinsic parameters			
				Translation (mm)		Rotation (°)	
Camera (#)		1	2	T_x	-873,63	Θ_x	-0,95
Distortions	K_1	1,91	-0,22				
	K_2	742,90	4043,47	T_y	-29,68	Φ_y	26,38
	K_3	0,40	4,26				
Plane center location (pixels)	X	587,14	635,53	T_z	67,67	Ψ_z	-0,06
	Y	408,46	485,61				

Table 1: Automatic system calibration was performed by using various images of a translated and rotated regular grid pattern within a bundle adjustment technique taken before, between and after the entire experiment. As a result, intrinsic and extrinsic camera parameters were obtained.

DATA ANALYSIS

For further analysis, the deformation in the out-of-plane direction (z) of every frame was assessed with dedicated algorithms implemented in Matlab (MathWorks, Natick, USA). First z-displacement was filtered with a 3D polynomial filter (Order was 1x1x3, and 3D window size was 10x10x15 in the x, y and time dimension respectively). The filter first provided out-of-plane displacement, but also velocity (first-derivative) and acceleration (second derivative) in the time domain in one filtering step (see Figure 2).

Although the paint was applied around the presumed trajectory of the artery as found by palpation, and although the trajectory was indicated with markings from a marker pen, arterial trajectory was estimated in an extra step by plotting maximal displacement during one heartbeat (see Figure 3.a and b), hypothesizing that the distension of the skin lying on top of tissues flanking the artery (muscle and larynx) is much smaller than distension of the skin lying on top of the artery. Then, the time domain was resampled 30 times in Matlab using a polyphase filter implementation [26], increasing sample frequency to 15000 samples/s. For further processing, the acceleration of the skin surface in the z-direction was considered (see Figure 1). For each pixel, the acceleration of the skin surface in the z-direction was analyzed for 2 specific local maxima, commonly used for detection of PWV: the maximum of z-acceleration of the surface, and the dicrotic notch [27] (see Figure 2). To detect these maxima, first a time window was manually delineated in one randomly chosen pixel. Then the local maximum was determined automatically in this window in every other pixel. After detection of the maxima, a visual inspection of accuracy of this approach was performed. Maps were made with the relative progress of the wave (see Figure 4). Secondly, the same characteristic time points were analyzed along the trajectory of the artery as described in previous paragraph (see Figure 3). The distance along the trajectory of the artery was plotted against the apparition in time of the local maxima, and from the slope of this relationship, the velocity of the wave, or the PWV was derived and its measurement error (ME) (see Figure 5). PWV was determined for every recorded pulse wave using two described algorithms (see Table 2 and 3). Strains were not subjected to any additional processing, and are mentioned for illustrative purposes only.

ULTRASOUND MEASUREMENTS

In order to compare the measured PWV values with parameters of the CCA, in each test subject arterial parameters were determined with US 1 to 3 weeks before the DIC measurements, performed by trained clinicians of the Department Cardiology of the University Hospital of Antwerp (UZA). All measurements were performed 3 times in a row. Test subjects were asked to remain sober 3 hours prior to the US measurement. Arterial parameters were used to estimate PWV, using the Bramwell-Hill equation: $PWV = \sqrt{A \cdot dP/(\rho \cdot dA)}$ (1), with A arterial cross-sectional area during diastole, dA difference in cross-sectional area between systole and diastole, ρ blood density, and dP pressure difference in the artery between systole and diastole [7].

The US and DIC methods were compared using a Bland-Altman (BA) analysis. For comparison, average of PWV pooled per individual, per method - and if applicable - per algorithm was used. For the BA analysis, a range of agreement was defined as mean bias ± 2 times standard deviation (SD) [28].

RESULTS

DIC

Out-of-plane displacement, velocity and acceleration of the CCA region were calculated in 3D, visualizing pulse wave propagation in the arterial segment. When the time domain of the signal is analyzed for specific points in the shape of the pulse wave, such as the maximum of acceleration, or the dicrotic notch, maps can be made of the relative progress of the pulse wave (see Figure 4). When the signal was

considered along the trajectory of the artery (see Figure 3), it can be observed that the pulse wave propagates in the segment (see Figure 6). Additionally, PWV could be calculated from these waveforms along the arterial segment (see Figure 5). $PWV_{acceleration}$ of individual heartbeats was found to be between (3,17±0,08) m/s and (5,32±0,05) m/s using the maximum of acceleration (reported as value ± ME), while average $PWV_{acceleration}$ per subject was found to be between (3,68±0,78) m/s and (5,09±0,22) m/s (reported as average ± SD). $PWV_{dicrotic\ notch}$ of individual heartbeats was found to be between (3,04±0,30) m/s and (6,23±0,66) m/s using the dicrotic notch (reported as value ± ME), while average $PWV_{dicrotic\ notch}$ per subject was found to be between (4,05±0,39) m/s and (5,19±0,53) m/s (reported as average ± SD). PWV as measured with DIC is summarized in Figure 7 and in table 2 and 3. Also, strains of the skin surface were calculated (see Figure 8 and 9).

ULTRASOUND

Blood pressure, intima media thickness (IMT), lumen diameter (D), distension, compliance coefficient (CC), distensibility coefficient (DC) and $PWV_{arterial\ parameters}$ were determined (see Table 4). PWV was found to be between 5,24±0,22 and 6,58±0,32 as calculated from the former parameters (see Figure 7 and Table 4). Since PWV values are calculated from averaged parameters with SD, PWV results are displayed as average with ME.

The BA analysis indicates that the 95% limits of agreement between the $PWV_{acceleration}$ compared to $PWV_{arterial\ parameters}$ ranged from -3,23 m/s to 0,77 m/s. The two methods do not consistently provide similar measures because there is a level of disagreement that includes discrepancies of up to -1,23 m/s. The BA analysis indicates that the 95% limits of agreement between the $PWV_{dicrotic\ notch}$ compared to $PWV_{arterial\ parameters}$ ranged from -2,85 m/s to 0,44 m/s. The two methods do not consistently provide similar measures because there is a level of disagreement that includes discrepancies of up to -1,20 m/s (see Figure 10).

Description		$PWV_{acceleration}$						$PWV_{dicrotic\ notch}$					
Measurement (#)		1			2			1			2		
Form		Minimum ± ME (m/s)	Maximum ± ME (m/s)	N	Minimum ± ME (m/s)	Maximum ± ME (m/s)	N	Minimum ± ME (m/s)	Maximum ± ME (m/s)	N	Minimum ± ME (m/s)	Maximum ± ME (m/s)	N
Subject (#)	1	3,76 ± 0,05	5,21 ± 0,12	3	3,70 ± 0,04	4,66 ± 0,07	3	4,27 ± 0,09	4,92 ± 0,12	2	3,54 ± 0,27	4,60 ± 0,12	2
	2	4,58 ± 0,25		1	3,17 ± 0,08	3,30 ± 0,03	2	4,27 ± 0,57		1	4,23 ± 0,05	4,49 ± 0,13	3
	3	4,81 ± 0,12	5,04 ± 0,09	2	5,19 ± 0,10	5,32 ± 0,05	2	4,54 ± 0,05	5,66 ± 0,05	2	4,97 ± 0,14	5,59 ± 0,31	2
	4	3,61 ± 0,34	4,14 ± 0,61	3	3,46 ± 0,27	3,80 ± 0,75	2	3,04 ± 0,30	5,14 ± 0,48	3	4,03 ± 0,44	6,23 ± 0,66	2
	5	4,91 ± 0,23	5,11 ± 0,18	2	5,20 ± 0,13		1	3,69 ± 0,17	3,99 ± 0,07	2	4,48 ± 0,05		1

Table 2: In each of the 5 test subjects PWV was determined twice (measurement 1 and 2) using two different algorithms ($PWV_{acceleration}$, and $PWV_{dicrotic\ notch}$). N indicates the amount of samples (heartbeats) for each (type of) measurement. Results are reported as maximum or minimum recorded value ± ME.

Description		Distension	
Measurement (#)		1	2
Form		Average ± SD (mm)	Average ± SD (mm)
Subject (#)	1	0,57 ± 0,34	0,60 ± 0,34
	2	0,27 ± 0,11	0,28 ± 0,16
	3	0,49 ± 0,14	0,64 ± 0,14
	4	0,27 ± 0,17	0,14 ± 0,13
	5	0,28 ± 0,12	0,44 ± 0,08

Table 3: In each of the 5 test subjects pixelwise average maximal distention was determined twice (measurement 1 and 2). Results are reported as average ± SD.

Subject (#)	Arterial parameters								
	IMT (mm)	N	D (mm)	N	Distension (mm)	N	PWV (m/s)	Relative difference (%)	
								acceleration	dicrotic notch
1	0,493±0,010	3	4,869±0,023	3	0,720±0,004	3	5,24±0,22	15,65	17,37
2	0,510±0,017	3	5,366±0,014	3	0,749±0,009	3	5,30±0,25	30,57	18,01
3	0,597±0,010	3	5,933±0,063	3	0,939±0,053	3	5,31±0,32	4,14	2,35
4	0,465±0,013	3	5,697±0,019	3	0,454±0,027	3	6,58±0,32	42,19	34,26
5	0,450±0,008	3	4,763±0,010	3	0,671±0,014	3	5,79±0,27	12,38	29,99

Table 4: In each of the 5 test subjects arterial parameters were determined with US. Wall thickness (IMT), lumen diameter (D), distension and $PWV_{arterial\ parameters}$ were determined. N indicates the amount of samples (heartbeats) for each (type of) measurement. Results are given as mean ± SD, except for PWV which is given as mean ± ME as it is calculated from several parameters with SD. The relative difference of the averaged PWV values as acquired with DIC is also given, using US as a reference.

DISCUSSION AND CONCLUSION

PWV is a clinical important marker for cardiovascular disease [8]. However, a golden standard for PWV detection is nonexistent at the moment [29]. Several approaches are available. Most methods focus on the PWV as measured between the carotid and the femoral artery. This approach measures PWV over the entire arterial system, while stiffness of central and peripheral arteries often differs [30]. Also, pulse wave form will change dramatically as measurement spots lie further apart, making it hard to define pulse transit time [31]. Moreover, estimating distance between measurement sites can introduce errors [32]. Finally, the patient is required to undress during measurements, which can be an issue in some parts of the world. Aforementioned reasons sparked interest in alternative ways of PWV determination.

Currently, determination of local PWV in the CCA attracts scientific attention. The CCA is an interesting target: the artery surfaces at an easily accessible place, distance between measurement sites can be readily measured, pulse wave will be minimally changed over short assessed distances, it is often affected by atherosclerosis, and augmented stiffness of the CCA is believed to cause hypertrophy of the heart due to wave reflections at the bifurcation [33].

Several non-invasive methods focus on PWV detection in the CCA, such as pulse wave imaging (PWI) [16], and laser Doppler vibrometry (LDV) [17,34]. Temporal resolution of reported PWI studies is often rather low (order of several 100 Hz), and LDV has a limited amount of measurement points (two measurement points when two regular LDV systems are used). Moreover, aiming the LDV systems exactly on top of the artery can be difficult.

In the present work, a DIC based non-contact method is presented for local PWV measurements in the CCA.

Temporal resolution 500 frames per second is achieved with current setup, equaling resolution acquired with US. For young healthy volunteers, where the PWV is low, this frame rate appears to be sufficient to detect PWV. However, in more clinically relevant populations, PWV will attain values of 13 m/s and more [8]. As such a higher frame rate will be required. Frame rates up to several kHz are within reach of modern high speed camera systems and will be subject of future research in order to attain validation in a population with higher PWV. Beat-to-beat variability defined as SD is as high as 1,56 m/s with DIC, and inter-session variability is as high as 1,35 m/s. Since local PWV measurements are not yet established as a screening method for cardiovascular disease, the question whether this is sufficient has yet to be answered. However, it can be expected that inter-session and beat-to-beat variability of the measurements will improve as frame rates increase.

Spatial resolution on the other hand is limited by factors such as resolution of the cameras at a specific sample frequency, position of the cameras, quality of the calibration step, characteristics of the lenses, coarseness of the speckle pattern, and correlation software [35]. An experimental or theoretical determination of the uncertainties on presented quantities was not performed during this experiment, since we were only interested in actual shape of the waveforms. However, post-hoc, we were able to achieve a resolution better than 0,015 mm.

Thanks to the achieved spatial resolution, it was possible to visualize the trajectory of the artery (see Figure 3) highlighting the importance of knowing the exact trajectory of the artery for local methods for PWV detection. Subsequently, PWV was assessed along this trajectory using known methods for pulse wave detection (Figure 5). Finally, maps of the relative progression of the wave could be made (see Figure 4).

However, it can be seen that the isolines in Figure 4 are non-equidistant. This could be explained by non-ideal elastic behavior and structural inhomogeneity in the trajectory of the artery or by artifacts due to undersampling and smoothing of the data, or by a combination of both. Also, the isolines appear to be slightly off-axis. The latter could be due to a slight tilt of the direction in which pulsation is at its maximum, and the z-axis of the measurement setup. To tackle this problem, coordinate systems could

be rotated, such that displacements in the z-direction are maximal (e.g. using principal component analysis (PCA)).

In order to validate the results, PWV values obtained with DIC measurements were compared with those obtained from US measurements as derived with the Bramwell-Hill equation (1) (see Figure 7). However, validation of local PWV measurements poses specific problems. The presented method is a time-of-flight approach, typically prone to errors introduced by wave reflections and changes in waveform over distance [12,29,33]. A single point measurement method could circumvent this problem. However, this would require extra information, such as local blood velocity profiles or local blood pressure profiles [36,37]. It can be expected that additional measurement equipment for this purpose would make the technique either impractical or invasive.

PWV Velocities as obtained from the Bramwell-Hill equation (1), however, give only an approximation of the "ground-truth" PWV, assuming ideal circumstances. PWV as calculated with this equation assumes absence of wave reflections, homogeneous mechanical parameters along the arterial trajectory, and zero blood velocity [38]. The dA and A from the equation are measured with a US probe, exerting mechanical pressure on the artery. It is plausible that this influences both arterial diameter, and mechanical properties of the artery. Also, dP is measured as difference between diastolic and systolic pressure as measured at the wrist. This pressure difference is expected to differ from the pressure at the CCA. Also ρ is based on literature values only.

Due to the small sample size, it is not possible to draw sound conclusions regarding reliability of the DIC method. Only a preliminary discussion of the precision, accuracy and reproducibility of the method will be given. Precision was already discussed earlier in terms of variability. A BA analysis was performed to assess accuracy. According to such an analysis, DIC estimates PWV on average lower than US, with wide limits of agreement considered from clinical perspective (see Figure 10). More research is needed to determine the accuracy of the DIC method in relation to the reference method, given that the cause of the bias is not fully understood. Possible explanations are a flaw in one of the methods, the entirely different nature of the methods, or the fact that PWV was not simultaneously recorded. Neither a correlation analysis comparing methods, nor an intra-class correlation analysis comparing measurement sessions was performed due to the small sample size. Therefore, reproducibility of the method remains to be investigated. Nevertheless, the values obtained from DIC and US are in the same order of magnitude, and they both are in the expected range considering medical background, age and gender of the test subjects, suggesting that values are realistic [7].

Additionally, strains were calculated, for illustrative purposes only (see Figure 8 and 9). Although strains were acquired in all test subjects, data could not be validated with another technique in this experiment. However, as calculation windows were varied, strain patterns remained very similar as assessed with visual inspection. Also, when more heartbeats were recorded in one session, patterns were periodical for separate heartbeats.

The extended spatial and temporal information become with the DIC opens possibilities for cardiovascular research purposes. Time-resolved, full-field information of the neck region is useful for creating strategies to measure PWV in a non-contact manner. It allows testing for algorithms to detect

progress of the wave optically. It allows testing for a robust measurement approach applicable on all types of patients. Moreover, it sheds light on the mechanical behavior of the neck region, and it can be used as reference for highly realistic FSI models of the CCA. Or, given that reliable FSI models are present, the arterial characteristics can be estimated through reverse engineering, revealing arterial characteristics.

Moreover, DIC can be further developed as a standalone diagnostic technique for PWV detection. One of the benefits of DIC is that the patient can remain fully dressed during measurements. Also, the actual measurement is non-contact; circumventing artifacts due to probe contact in tonometry and US based applications. The data allow post-hoc determination of the arterial trajectory. Additionally, performing a measurement (application of the speckle pattern, and recording several heartbeats with DIC) is not likely to take more than 10 minutes when executed by a skilled technician.

However, the technique also has its limitations: time-of-flight methods for PWV detection are typically sensitive to the effect of wave reflections. Also, special attention is required for the preparation of the surface: the contrast between background and speckles has to be as high as possible, and speckles ideally are as small as possible, and evenly distributed in a random fashion, requiring some experience. Moreover, setup of the camera systems, calibration, and especially processing of the data is time consuming making real-time analysis unfeasible at the moment.

Additionally, in order for an object to be studied, visual access from the camera(s) is required over the entire surface, limiting extensive miniaturization of the setup. Also, in order to achieve focus over the entire object, high illumination is required when some relief or substantial out-of-plane displacements are at play, especially at short shutter times. Shadows and blind corners, caused e.g. by wrinkles, hairs, impurities of the skin, and skin folds will inevitably lead to artifacts. Current measurements were performed in healthy young males with no facial hear, low BMI and low PWV. However, it remains to be tested how DIC will perform on skin with skin folds, wrinkles or when prominent presence of facial hair. In order to make the skin surface smoother, a white ground layer capable of filling cracks and pores could be used, and patients could be asked to shave themselves before a consultation. Also, pulsation could be hard to detect when a fat content in the neck is high, or when blood pressure is very low. In this case, required sensitivity of the technique could be acquired with a finer speckle pattern. However, the limits of the technique remain to be explored in future work.

Some measures could be made to make the technique more applicable and more user-friendly. The ground layer could be enriched with a fluorescent molecule. By illuminating the patch with a laser and recording with an appropriate filter for the camera, the use of large illumination equipment can be avoided. Or, in order to skip the process of applying 2 layers of paint, a printed fluorescent pattern could be applied on the skin e.g. with a rub-on tattoo. The cameras could be triggered by ECG to reduce the amount of images to be analyzed to a minimum. If 3D information is not required, variants of the technique can be developed with only one camera and even a projected pattern, reducing cost, reducing required computational power, and increasing user friendliness of the setup. In the presence of background movements, principal strains could be used for estimation of PWV.

It is obvious that the time-resolved, full-field assessment of movement and strains of surfaces creates opportunities for all kinds of biological and non-biological applications. The technique requires at most 2 cameras, a bright light source, and the application of some paint, and is physiologically harmless. Moreover, a setup is relatively small and lightweight, and as such very versatile and mobile. There are no interferometric stability requirements rendering this technique usable for applications outside the lab. Consequently, this technique has the potential to find its way in other biological studies where motion of surfaces are to be assessed as a function of time, for example study of the movement of eardrums for different frequencies and amplitudes [39], dynamics of leaf growth, modeling of biting mechanics of stag beetles, and assessing complex biomaterials in general, amongst other possible applications.

ACKNOWLEDGEMENTS

We acknowledge the Research Foundation of Flanders (FWO-Vlaanderen) for financial support.

LITERATURE

[1] H. Schreier, J.-J. Orteu, and M. a. Sutton, “Image Correlation for Shape, Motion and Deformation Measurements,” Springer US, Boston, MA (2009) [doi:10.1007/978-0-387-78747-3].

[2] T. Schmidt, J. Tyson, and K. Galanulis, “FULL-FIELD DYNAMIC DISPLACEMENT AND STRAIN MEASUREMENT USING ADVANCED 3D IMAGE CORRELATION PHOTOGRAMMETRY: PART 1,” *Exp. Tech.* **27**(3), 47–50 (2003) [doi:10.1111/j.1747-1567.2003.tb00115.x].

[3] J. Tyson, T. Schmidt, and K. Galanulis, “BIOMECHANICS DEFORMATION AND STRAIN MEASUREMENTS WITH 3D IMAGE CORRELATION PHOTOGRAMMETRY,” *Exp. Tech.* **26**(5), 39–42 (2002) [doi:10.1111/j.1747-1567.2002.tb00083.x].

[4] M. A. Sutton, X. Ke, S. M. Lessner, M. Goldbach, M. Yost, F. Zhao, and H. W. Schreier, “Strain field measurements on mouse carotid arteries using microscopic three-dimensional digital image correlation.,” *J. Biomed. Mater. Res. A* **84**(1), 178–190 (2008) [doi:10.1002/jbm.a.31268].

[5] P. Sztefek, M. Vanleene, R. Olsson, R. Collinson, A. A. Pitsillides, and S. Shefelbine, “Using digital image correlation to determine bone surface strains during loading and after adaptation of the mouse tibia.,” *J. Biomech.* **43**(4), 599–605 (2010) [doi:10.1016/j.jbiomech.2009.10.042].

[6] J. Soons, P. Lava, D. Debruyne, and J. Dirckx, “Full-field optical deformation measurement in biomechanics: digital speckle pattern interferometry and 3D digital image correlation applied to bird beaks.,” *J. Mech. Behav. Biomed. Mater.* **14**, 186–191 (2012) [doi:10.1016/j.jmbbm.2012.05.004].

[7] W. R. Milnor, *Hemodynamics*, p. 390, Williams & Wilkins (1982).

[8] S. Laurent, P. Boutouyrie, R. Asmar, I. Gautier, B. Laloux, L. Guize, P. Ducimetiere, and A. Benetos, “Aortic Stiffness Is an Independent Predictor of All-Cause and Cardiovascular Mortality in Hypertensive Patients,” *Hypertension* **37**(5), 1236–1241 (2001) [doi:10.1161/01.HYP.37.5.1236].

[9] K. Matthys and P. Verdonck, “Development and modelling of arterial applanation tonometry: a review.,” *Technol. Health Care* **10**(1), 65–76 (2002).

[10] J. Calabia, P. Torguet, M. Garcia, I. Garcia, N. Martin, B. Guasch, D. Faur, and M. Vallés, “Doppler ultrasound in the measurement of pulse wave velocity: agreement with the Complior method.,” *Cardiovasc. Ultrasound* **9**(1), 13 (2011) [doi:10.1186/1476-7120-9-13].

[11] M. De Melis, U. Morbiducci, L. Scalise, E. P. Tomasini, D. Delbeke, R. Baets, L. M. Van Bortel, and P. Segers, “A noncontact approach for the evaluation of large artery stiffness: a preliminary study.,” *Am. J. Hypertens.* **21**(12), 1280–1283 (2008) [doi:10.1038/ajh.2008.280].

[12] E. Hermeling, K. D. Reesink, A. P. G. Hoeks, and R. S. Reneman, “Potentials and pitfalls of local PWV measurements.,” *Am. J. Hypertens.* **23**(9), 934; author reply 935 (2010) [doi:10.1038/ajh.2010.123].

[13] P. Boutouyrie, S. Laurent, X. Girerd, A. Benetos, P. Lacolley, E. Abergel, and M. Safar, “Common Carotid Artery Stiffness and Patterns of Left Ventricular Hypertrophy in Hypertensive Patients,” *Hypertension* **25**(4), 651–659 (1995) [doi:10.1161/01.HYP.25.4.651].

[14] S. C. Millasseau, A. D. Stewart, S. J. Patel, S. R. Redwood, and P. J. Chowienczyk, “Evaluation of carotid-femoral pulse wave velocity: influence of timing algorithm and heart rate.,” *Hypertension* **45**(2), 222–226 (2005) [doi:10.1161/01.HYP.0000154229.97341.d2].

[15] S. I. Rabben, N. Stergiopulos, L. R. Hellevik, O. A. Smiseth, S. Slørdahl, S. Urheim, and B. Angelsen, “An ultrasound-based method for determining pulse wave velocity in superficial arteries.,” *J. Biomech.* **37**(10), 1615–1622 (2004) [doi:10.1016/j.jbiomech.2003.12.031].

[16] J. Vappou, J. Luo, and E. E. Konofagou, “Pulse wave imaging for noninvasive and quantitative measurement of arterial stiffness in vivo.,” *Am. J. Hypertens.* **23**(4), 393–398 (2010) [doi:10.1038/ajh.2009.272].

[17] A. Campo, P. Segers, and J. Dirckx, “Laser Doppler vibrometry for in vivo assessment of arterial stiffness,” in *2011 IEEE Int. Symp. Med. Meas. Appl.*, pp. 119–121, IEEE (2011) [doi:10.1109/MeMeA.2011.5966691].

[18] Z. Zhang, “A Flexible New Technique for Camera Calibration,” *IEEE Trans. Pattern Anal. Mach. Intell.* **22**(11), 1330–1334 (2000) [doi:10.1109/34.888718].

[19] B. Triggs, “Detecting Keypoints with Stable Position, Orientation, and Scale under Illumination Changes,” in *Comput. Vis. - ECCV 2004* **3024**, pp. 100–113 (2004) [doi:10.1007/978-3-540-24673-2_9].

[20] P. Lava, “Assessment of Measuring Errors in Strain Fields Obtained via DIC on Planar Sheet Metal Specimens with a Non-Perpendicular Camera Alignment,” *Appl. Mech. Mater.* **70**, 165–170 (2011).

[21] P. Lava, S. Cooreman, S. Coppieters, M. De Strycker, and D. Debruyne, “Assessment of measuring errors in DIC using deformation fields generated by plastic FEA,” *Opt. Lasers Eng.* **47**(7-8), 747–753 (2009) [doi:10.1016/j.optlaseng.2009.03.007].

[22] B. Pan, K. Qian, H. Xie, and A. Asundi, “Two-dimensional digital image correlation for in-plane displacement and strain measurement: a review,” *Meas. Sci. Technol.* **20**(6), 062001 (2009) [doi:10.1088/0957-0233/20/6/062001].

[23] R. Keys, “Cubic convolution interpolation for digital image processing,” *IEEE Trans. Acoust.* **29**(6), 1153–1160 (1981) [doi:10.1109/TASSP.1981.1163711].

[24] H. A. Bruck, S. R. McNeill, M. A. Sutton, and W. H. Peters, “Digital image correlation using Newton-Raphson method of partial differential correction,” *Exp. Mech.* **29**(3), 261–267 (1989) [doi:10.1007/BF02321405].

[25] G. T. Mase, *Continuum mechanics for engineers*, second edi, in *New York*, second edi, p. 380, CRC Press, New York (1999).

[26] A. (Massachusetts I. of T. Oppenheim, R. (Georgia I. of T. Schafer, and J. (University of M. D. Buck, *Discrete-Time Signal Processing*, 2nd ed., M. Horton, Ed., p. 896, Prentice-Hall, Inc., New Jersey (1999).

[27] E. Hermeling, K. D. Reesink, L. M. Kornmann, R. S. Reneman, and A. P. Hoeks, “The dicrotic notch as alternative time-reference point to measure local pulse wave velocity in the carotid artery by means of ultrasonography.,” *J. Hypertens.* **27**(10), 2028–2035 (2009) [doi:10.1097/HJH.0b013e32832f5890].

[28] J. M. Bland and D. Altman, “Statistical methods for assessing agreement between two methods of clinical measurement,” *Lancet*, 307–310 (1986).

[29] E. Hermeling, K. D. Reesink, R. S. Reneman, and A. P. G. Hoeks, “Measurement of local pulse wave velocity: effects of signal processing on precision.,” *Ultrasound Med. Biol.* **33**(5), 774–781 (2007) [doi:10.1016/j.ultrasmedbio.2006.11.018].

[30] J. Sugawara, K. Hayashi, T. Yokoi, M. Y. Cortez-Cooper, A. E. DeVan, M. A. Anton, and H. Tanaka, “Brachial-ankle pulse wave velocity: an index of central arterial stiffness?,” *J. Hum. Hypertens.* **19**(5), 401–406 (2005) [doi:10.1038/sj.jhh.1001838].

[31] C.-W. Chang, J.-M. Chen, W.-K. Wang, and Y.-Y. L. Wang, “PWV measurement influenced by distance between two recording sites.,” *Am. J. Hypertens.* **24**(3), 250, American Journal of Hypertension, Ltd (2011) [doi:10.1038/ajh.2010.245].

[32] S. A. M. Huybrechts, D. G. Devos, S. J. Vermeersch, D. Mahieu, E. Achten, T. L. M. de Backer, P. Segers, and L. M. van Bortel, “Carotid to femoral pulse wave velocity: a comparison of real travelled aortic path lengths determined by MRI and superficial measurements.,” *J. Hypertens.* **29**(8), 1577–1582 (2011) [doi:10.1097/HJH.0b013e3283487841].

[33] P. Segers, J. Mynard, L. Taelman, S. Vermeersch, and A. Swillens, “Wave reflection: Myth or reality?,” *Artery Res.* **6**(1), 7–11 (2012) [doi:10.1016/j.artres.2012.01.005].

[34] Y. Li, P. Segers, J. Dirckx, and R. Baets, “On-chip laser Doppler vibrometer for arterial pulse wave velocity measurement.,” *Biomed. Opt. Express* **4**(7), 1229–1235 (2013) [doi:10.1364/BOE.4.001229].

[35] R. H. Pritchard, P. Lava, D. Debruyne, and E. M. Terentjev, “Precise determination of the Poisson ratio in soft materials with 2D digital image correlation,” 1–14 (2013).

[36] A. W. Khir, A. O’Brien, J. S. Gibbs, and K. H. Parker, “Determination of wave speed and wave separation in the arteries.,” *J. Biomech.* **34**(9), 1145–1155 (2001).

[37] J. Feng and A. W. Khir, “Determination of wave speed and wave separation in the arteries using diameter and velocity.,” *J. Biomech.* **43**(3), 455–462 (2010) [doi:10.1016/j.jbiomech.2009.09.046].

[38] W. W. Nichols, M. F. O’Rourke, C. Vlachopoulos, A. P. Hoeks, and P. D. CON, *McDonald’s Blood Flow in Arteries: Theoretical, Experimental and Clinical Principles*, p. 755, Hodder Arnold Publishers (2011).

[39] J. Aernouts, J. R. M. Aerts, and J. J. J. Dirckx, “Mechanical properties of human tympanic membrane in the quasi-static regime from in situ point indentation measurements.,” *Hear. Res.* **290**(1-2), 45–54, Elsevier B.V. (2012) [doi:10.1016/j.heares.2012.05.001].

LIST OF FIGURES

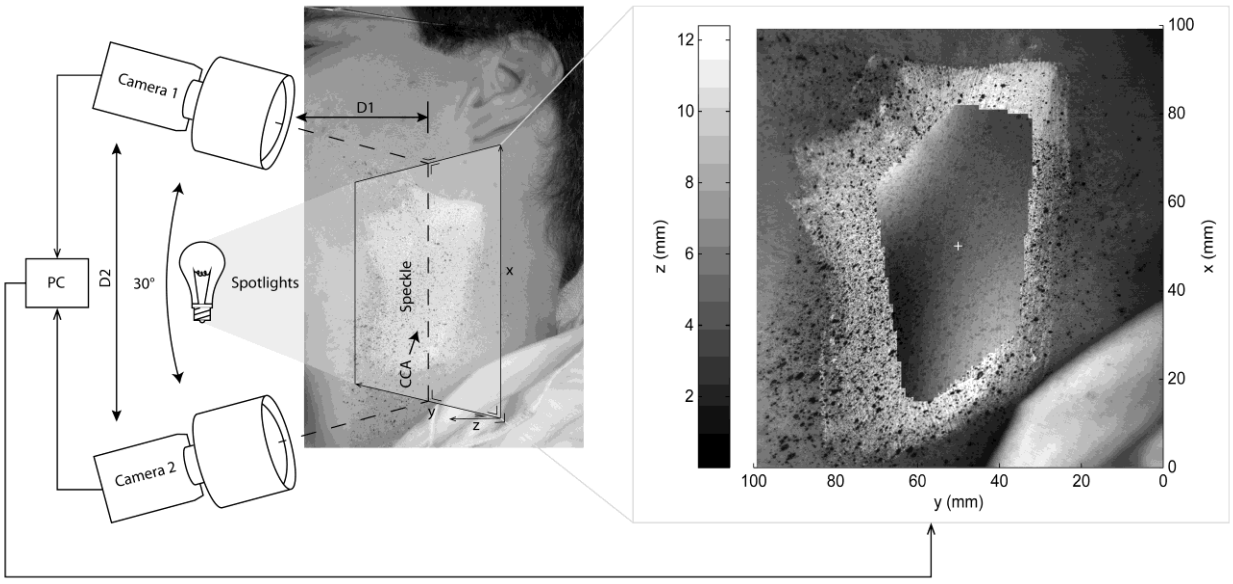

Figure 1: the experimental setup with the relative position of the stereo system and the measurement area (left pane). X and y axes define the in plane components, out-of-plane components are reported in the right pane as z-axis. A Stereo system with two cameras with an opening angle of approximately 30° was used. Approximate distance D1 between cameras and subject was 1 m, approximate mutual distance between cameras was 0,5 m. High power LEDs fed with DC to avoid flickering illuminate the sample. In the neck in the region around the CCA, a ground layer of white paint is applied, covered with a black speckle pattern. The trajectory of the artery is indicated with a black arrow. The white cross in the right pane refers to Figure 2.

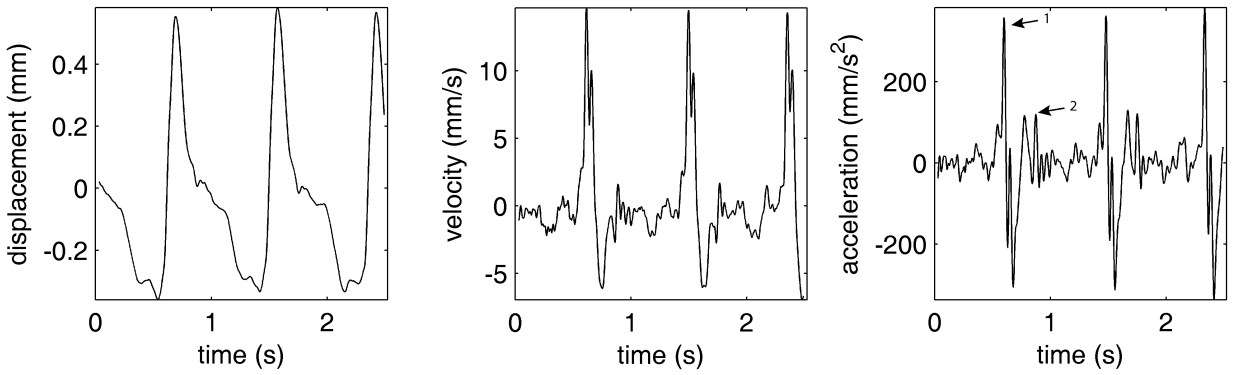

Figure 2: After smoothing, for each pixel displacement, velocity and acceleration in the z-direction was acquired by the filtering step as described. 3 quantities are illustrated here as a function of time for an arbitrary point on the assessed surface (measurement location is indicated with a white cross in previous Figure 1). Characteristic time points of the wave are indicated with numbers in the rightmost pane (z-acceleration): maximum of acceleration (1) and dicrotic notch (2).

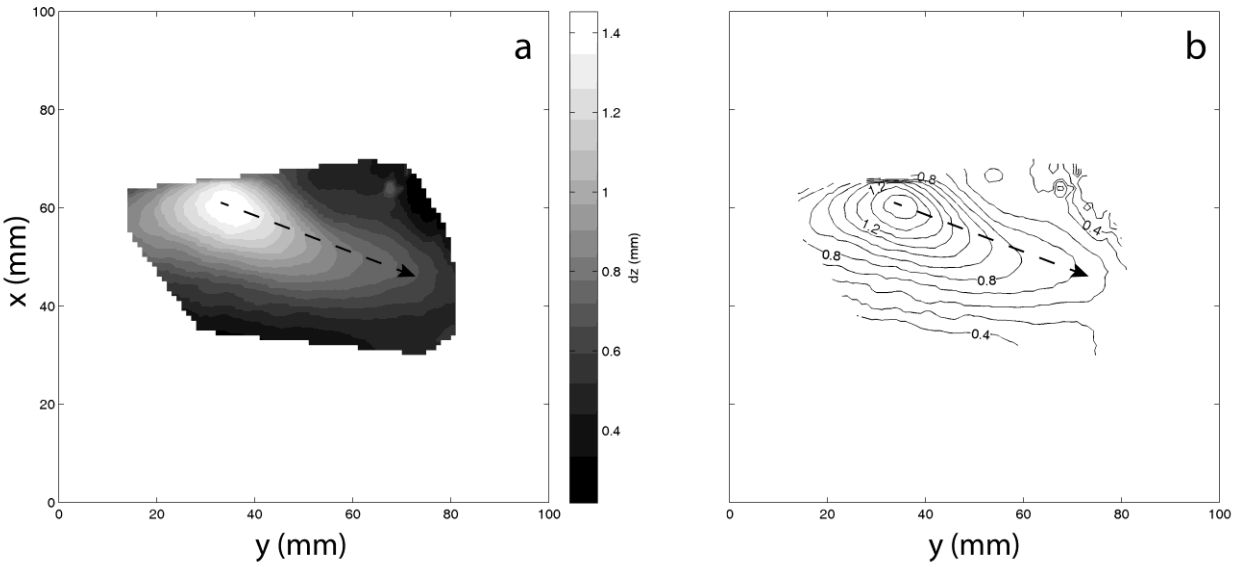

Figure 3: Arterial trajectory was estimated in an extra step by rendering maximal displacement during one heartbeat, hypothesizing that the distension of the skin lying on top of tissues flanking the artery (muscle and larynx) is much smaller than distension of the skin lying on top of the artery. As a consequence, a clear longitudinal region can be seen, highlighting the trajectory of the artery. In the left pane, the maximal distension is shown in one heartbeat, in the right pane, a contour plot is shown of the same data. Isolines are in mm. The trajectory of the artery is indicated with a black arrow. In the upper right corner of the figures, some noise can be seen

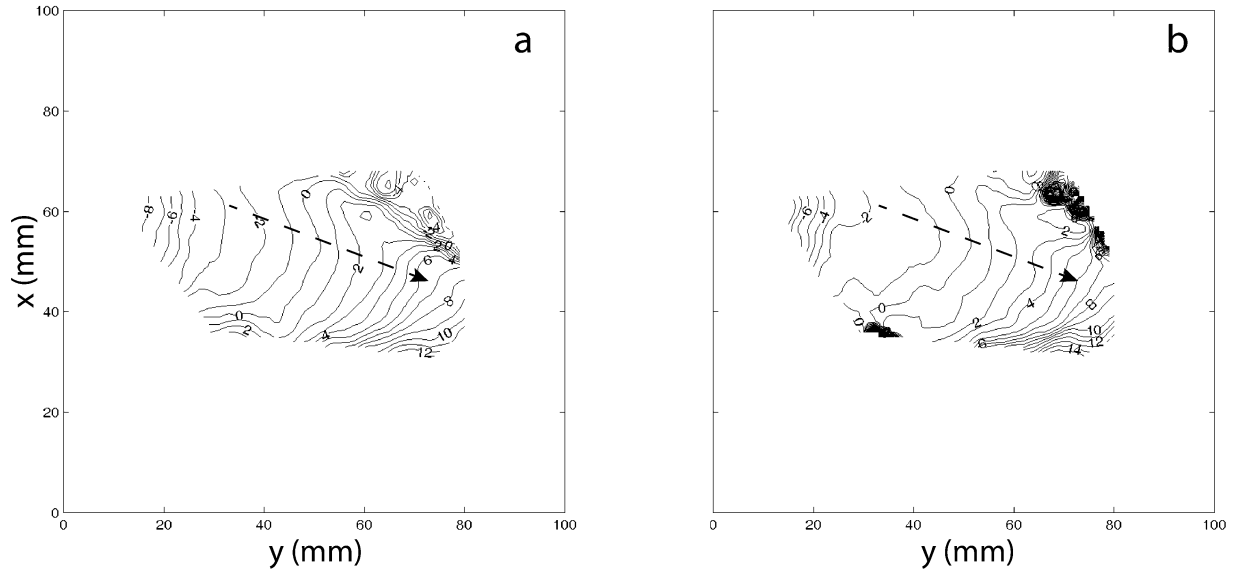

Figure 4: For each pixel, time domain was analyzed for characteristic time points in the shape of each recorded pulse wave, in order to track the wave and determine its velocity. This was done for the entire measured domain for 2 different characteristic time points commonly used in PWV detection: the maximum of z-acceleration of the surface (a), and the dicrotic notch (b). Contour plots were made using

the relative progress of these time points, thus displaying the progress of the wave. Again, the trajectory of the artery is indicated with a black arrow. Isolines are in ms. In the upper right corner of the figures, some noise is present.

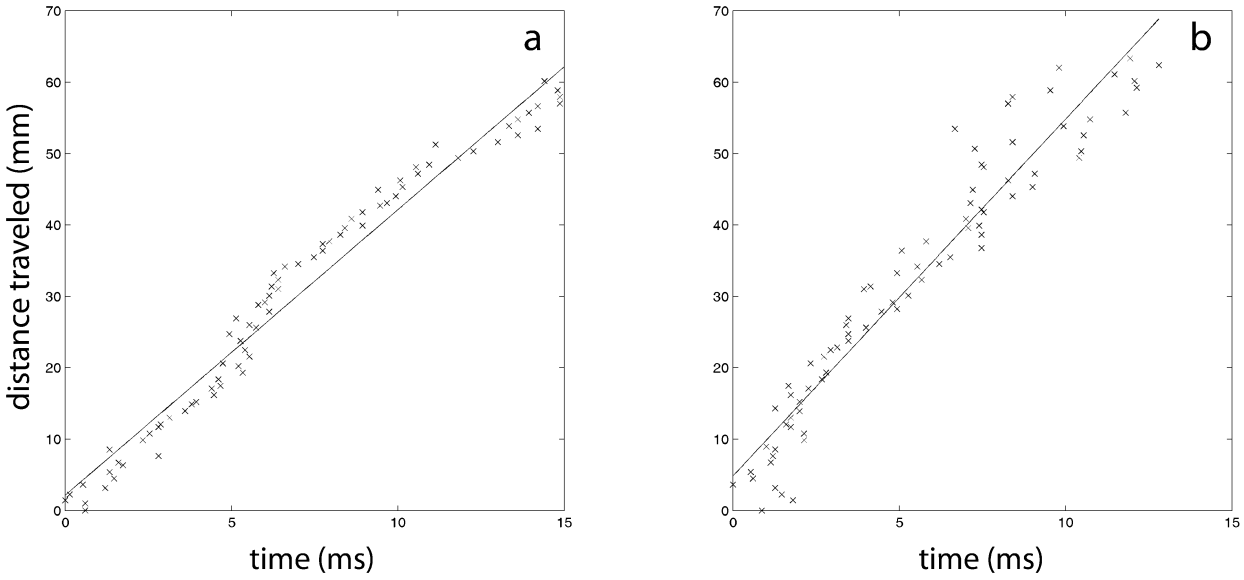

Figure 5: The trajectory was found as explained above. The trajectory is displayed in Figure 3. The distance along the trajectory of the artery was plotted against the moment of appearance of the characteristic time points, and from the slope of this relationship, the velocity of the wave, or the PWV was derived. In the left pane (a), PWV is calculated finding the maximum of z-acceleration, and in the right pane (b), PWV is calculated by finding the dicrotic notch. In this particular example we find for $PWV_{acceleration}$: $PWV_{acceleration}$ = (4,00 ± 0,04) m/s, R2 = 0,97; and for $PWV_{dicrotic\ notch}$: $PWV_{dicrotic\ notch}$ = (5,00 ± 0,09) m/s, R2 = 0,92.

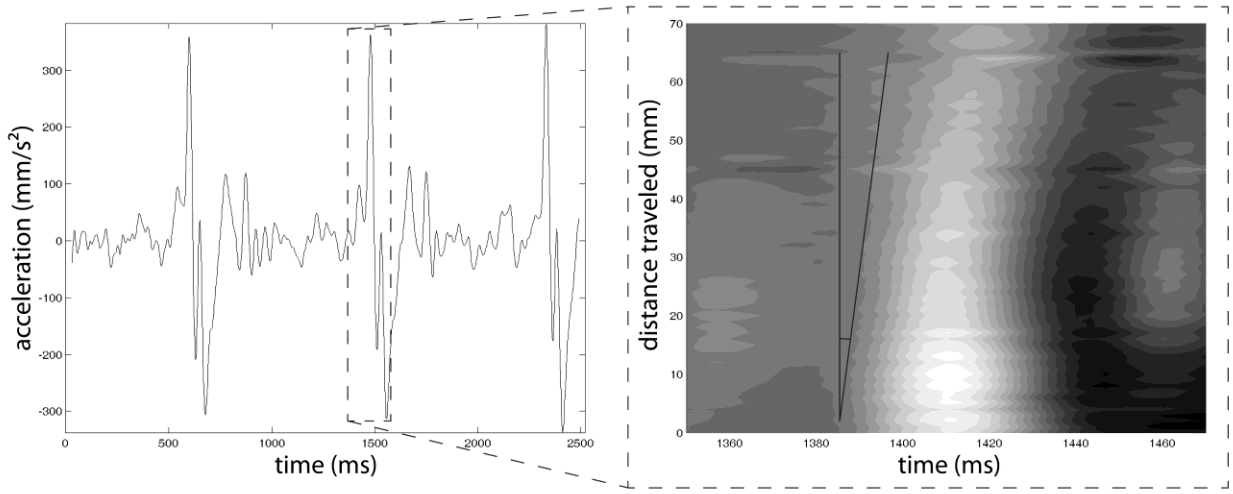

Figure 6: When the z-acceleration is considered along the trajectory of the artery, the propagation of the pulse wave can be tracked by observing characteristic time points such as the maximum of acceleration

or the dicrotic notch. In this figure, the left pane displays a typical profile of the z-acceleration of the skin above the CCA. 3 heartbeats can be discerned. The right pane shows a close-up (close-up window is indicated with dashed box) of the region around the maximum of z-acceleration of the second heartbeat in the left pane for a series of points along the trajectory of the artery. The horizontal axis indicates time; the vertical axis indicates distance traveled along the arterial trajectory by the pulse wave. The angle displayed on the right pane illustrates propagation of the maximum of acceleration along the trajectory of the artery.

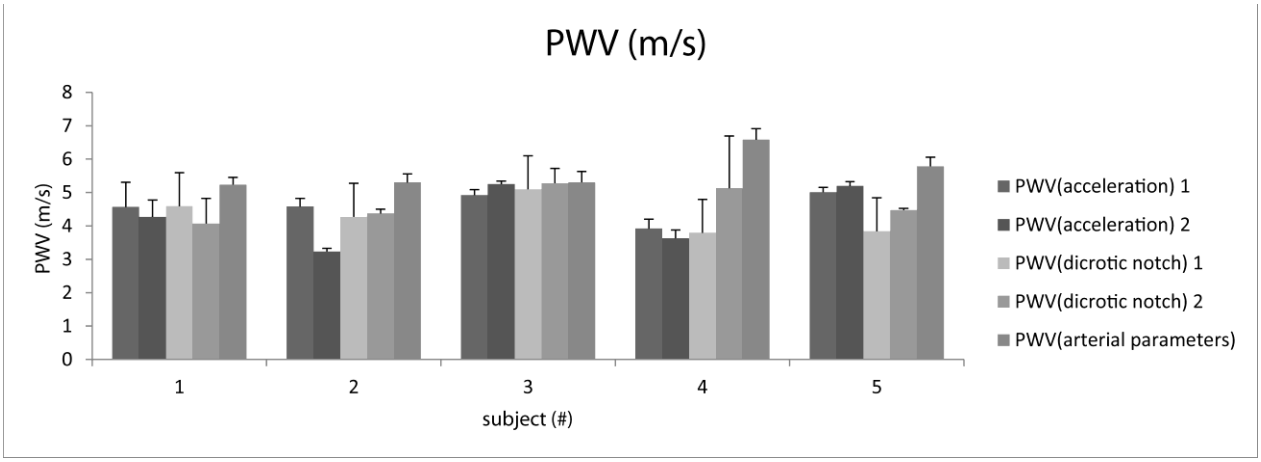

Figure 7: PWV was determined using three different detection methods: using the maximum of acceleration, using the dicrotic notch, and using arterial parameters in combination with the Bramwell-Hill equation (1). PWV values are represented as average PWV per subject, per measurement.

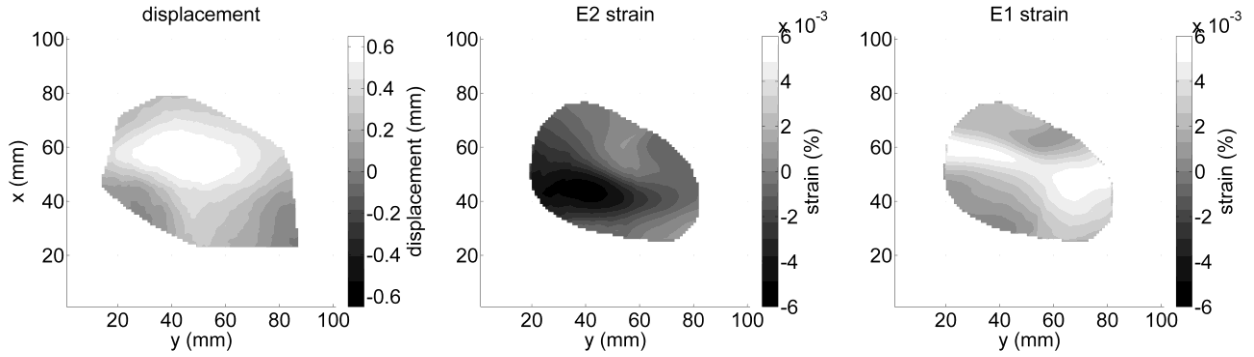

Figure 8: Strains of the skin on top of the CCA were calculated. Here, a z-displacement profile from an arbitrary point on the skin is given, as well as the principal strains E1 and E2 for the same point. Strain profiles were appeared very similar within the same test subject, and for different calculation windows. Diamonds indicate points compared in Figure 9. The upper pane displays displacement, the middle pane displays strain E1 and the lower pane displays strain E2.

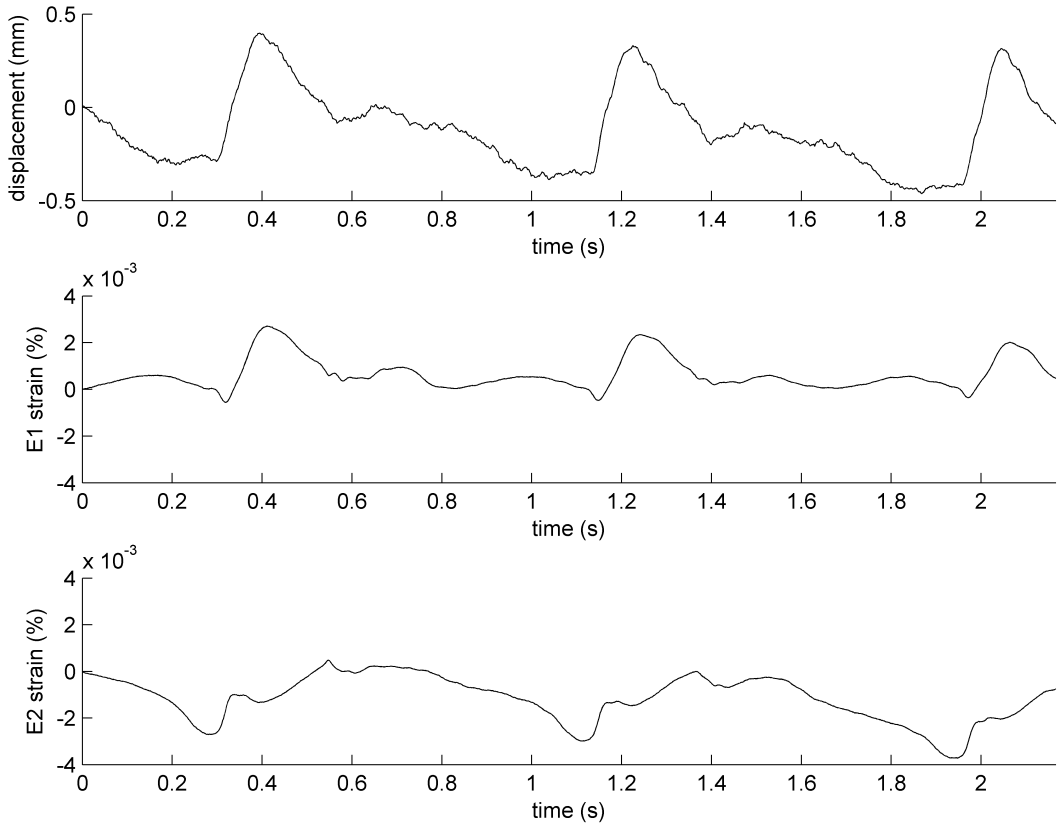

Figure 9: Full field strains were calculated for the skin above the CCA. Here strains and z-displacements are displayed between measurement points as indicated in Figure 8. The left pane displays displacement, the middle pane displays strain E1 and the right pane displays strain E2. In the plane displaying displacement and in the pane displaying E1 strain, a clear longitudinal region is highlighted along the trajectory of the artery.

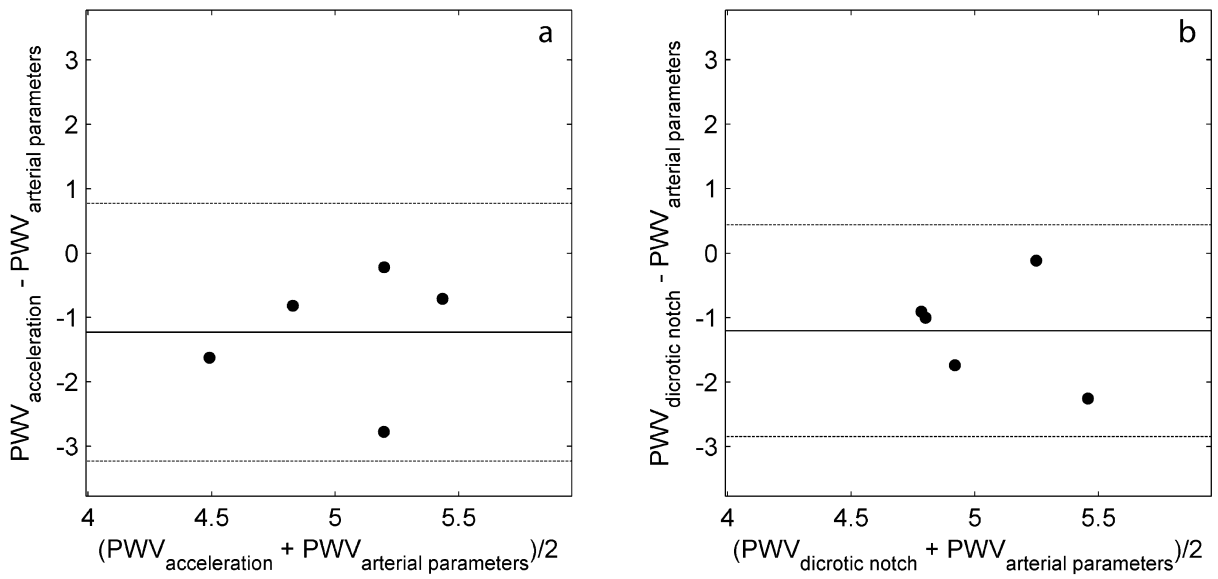

Figure 10: A BA analysis to assess the level of agreement between the $PWV_{acceleration}$ compared to $PWV_{arterial\ parameters}$ (left panel) and between $PWV_{dicrotic\ notch}$ compared to $PWV_{arterial\ parameters}$ (right panel). A range of agreement was defined as mean bias (full line) ± 2 times SD (dashed line).